C. R. Palevol 17 (2018) 17–32

Contents lists available at ScienceDirect

Comptes Rendus Palevol

www.sciencedirect.com

Human Palaeontology and Prehistory

The Kocabaş hominin (Denizli Basin, Turkey) at the crossroads of Eurasia: New insights from morphometric and cladistic analyses

L'homininé de Kocabaş (bassin de Denizli, Turquie) au carrefour de l'Eurasie : nouvelles données obtenues à partir d'analyses morphométriques et cladistiques

Amélie Vialet[a], Sandrine Prat[b], Patricia Wils[c], Mehmet Cihat Alçiçek[d]

[a] *UMR 7194, CNRS, Muséum national d'histoire naturelle, UPVD CERP de Tautavel, 1, rue René-Panhard, 75013 Paris, France*
[b] *UMR 7194, CNRS, Muséum national d'Histoire naturelle, UPVD, Musée de l'Homme, 17, place du Trocadéro, 75116 Paris, France*
[c] *UMS 2700, outils et méthodes de la systématique intégrative, Muséum national d'Histoire naturelle, 43, rue Buffon, 75005 Paris, France*
[d] *Department of Geology, Pamukkale University, 20070 Denizli, Turkey*

ARTICLE INFO

Article history:
Received 4 June 2017
Accepted after revision 21 November 2017

Handled by Yves Coppens

Keywords:
Hominin
Turkey
Morphometry
Cladistics
Out of Africa

Mots clés :
Homininé
Turquie
Morphométrie
Cladistique
Expansion hors d'Afrique

ABSTRACT

The Kocabaş skullcap (Denizli Basin), dated between 1.2 and 1.6 Ma, is the only ancient hominin fossil from Turkey and is part of discussions focusing on the first settlement outside the African continent. Our morphometric study tends to link this specimen with the African fossils, *Homo ergaster* and early *Homo erectus*, and to distinguish it from the specimens from Dmanisi and Asian *Homo erectus*. These results are confirmed by a cladistic analysis, which shows a separation of Kocabaş from the Eurasian clade comprising the Dmanisi hominins and grouping it with the African fossils dated to around 1 Ma (KNM-OL 45500, Daka-Bouri BouVP2/66, Buia UA31). As in the Kocabaş fossil, the divergence of the frontal bone is not very marked on these latter fossils and the temporal lines are separated on the parietal bone. The Kocabaş skull seems to point to a different evolutionary history than that of the Dmanisi fossils, and could reflect a later "out-of-Africa" expansion.

RÉSUMÉ

Seul fossile d'homininé ancien en Turquie, la calotte crânienne de Kocabaş (bassin de Denizli), datée entre 1,2 et 1,6 Ma, s'inscrit dans la discussion sur les premiers peuplements en dehors du continent africain. Notre étude morphométrique tend à le rapprocher des fossiles africains, *Homo ergaster* et *Homo erectus* récents, et à le distinguer des spécimens de Dmanissi et des *Homo erectus* asiatiques. Ces résultats sont confirmés par une analyse cladistique qui montre une séparation du fossile de Kocabaş du clade eurasiatique qui inclut les homininés de Dmanissi, et le regroupe avec les fossiles africains datés autour d'1 Ma (KNM-OL 45500, Daka-Bouri BouVP2/66, Buia UA31). Ces derniers partagent avec Kocabaş une divergence de l'os frontal peu marquée et une séparation des lignes temporales sur l'os pariétal. Le crâne de Kocabaş semble témoigner d'une histoire évolutive différente de celle des fossiles de Dmanissi, qui pourrait correspondre à une expansion hors d'Afrique plus tardive.

E-mail address: amelie.vialet@mnhn.fr (A. Vialet).

https://doi.org/10.1016/j.crpv.2017.11.003
1631-0683/

1. Introduction

Several hominin fossils are known from Africa after 7 Ma, when the first early *Homo* is recorded at 2.8 Ma (Villmoare et al., 2015). There is a significant time lag of about 1 Ma between Africa and Eurasia, where the first human fossils are dated to 1.77 Ma at the site of Dmanisi in Georgia. This latter is the earliest known direct evidence of the "out-of-Africa" expansion. Based on lithic assemblages discovered in Asia, these first waves of settlement could be considerably older than 2 Ma (Prat, 2018, this issue). However, these discoveries remain scarce. In this context, the Kocabaş skull, from the Denizli Basin in Turkey, provides important evidence of early human presence in the Middle East, or an "out-of-Africa" expansion along the Levantine corridor, and possible dispersal toward Europe – via the Bosphorus Strait – and toward Asia – across mountainous territories such as the Taurus, Zagros, and the Caucasus. Although the Kocabaş skullcap is very fragmented, it fills a paleoanthropological gap between 1.6 and 1.2 Ma, not only in Africa but also in Eurasia. Indeed, there is no fossil between OH9 from Olduvai in Tanzania and the one-million-year-old *Homo erectus*-like hominins from East Africa (KNM-OL 45500, Daka-Bouri BouVP2/66, Buia UA 31). In Europe, apart from the deciduous tooth from the Orce Basin dated to 1.4 Ma (Toro-Moyano et al., 2013), the oldest human fossils are from the Atapuerca–Sima del Elefante site dated to 1.2 Ma (Carbonell et al., 2008).

The goal of this paper is, on one hand, to characterize morphometrically the Kocabaş fossil and, on the other hand, to test its link with other Pleistocene hominins from Africa and Asia using cladistic analysis. The main question is to establish whether the Turkish hominin, found at the crossroads of Africa and Asia between 1.6 and 1.2 Ma, is indeed closer to African or Asian specimens.

2. Background

The Kocabaş fossil was discovered in 2002 by one of us (M.C.A.) in one of the quarries in the Denizli Basin (Alçiçek and Alçiçek, 2014). The small skull was sliced by the blades used to cut blocks in this travertine quarry. Although the discovery of the skull was accidental, associated fauna is abundant in the find horizon (Alçiçek, 2014, Boulbes et al., 2014). This fossiliferous horizon from which the Kocabaş fossil comes from, is identified as the upper travertine (UT) (Lebatard et al., 2014a, 2014b), which was the only quarried travertine at the time of discovery in 2002, and the only unit to have yielded paleontological material up until now.

The stratigraphic and chronological context of the UT bearing the hominin skull and an abundant Upper Villafranchian fauna were comprehensively defined during the field missions in 2011 and 2012. This fieldwork has been focused on the deposits from the Faber Quarry where the succession reaches a depth of over 90 m and contains preserved levels comparable to those from which the fossils were extracted in 2002 within the UT. This UT unit is situated stratigraphically between two fluviatile levels. The results obtained from $^{26}Al/^{10}Be$ cosmogenic nuclides analysis on the overlying and underlying fluviatile conglomerate levels (Lebatard et al., 2014a, 2014b) indicate an age of 1.1 Ma and 1.6 Ma respectively, setting a chronological bracket between these two dates for the Kocabaş fauna and the human fossil. The magnetostratigraphy for the whole sequence of the deposits (Khatib et al., 2014) allows a correlation of the base of the upper fluvial unit (normal polarity) with the Cobb Mountain excursion, dated to 1.22 Ma. Moreover, the biochronology of the fauna *Archidiskodon merionalis meridionalis* (*Elephantidae*) and *Palaeotragus* (*Giraffidae*) associated with the skull (Boulbes et al., 2014) confirms this chronological framework between 1.2 and 1.6 Ma.

No lithic artefacts are strictly associated with the human and animal fossils from the UT of the Denizli Basin. Archaeological prospection in the surrounding terraces has just started recently (Maddy et al., 2015; Aytek *comm. pers.*), leading to the discovery of lithic artefacts, mostly on the surface. More generally, few Lower Palaeolithic sites are known in Turkey (Dinçer, 2016) and none are as old as the Kocabaş locality. We have no evidence for the moment to ascertain whether at 1.2/1.6 Ma, the technological mode could be related to Oldowan or Acheulean technocomplexes. However, the Dursunlu site (Güleç et al., 2009) and Yarimburgaz Cave (Howell et al., 1996) have yielded stone flakes. The open-air site of Kaletepe Deresi 3 attested to the presence of well-shaped handaxes made of obsidian (Slimak et al., 2004, 2008) dated to the middle Pleistocene (Tryon et al., 2009). Some handaxes were discovered in the lower levels of the Karain E Cave (Taşkıran, 2008, Taşkıran, 2018 this issue). At this site, the Mousterian industry is well represented in the upper levels in association with 20 fragmentary Neandertal-like human remains (Chevalier et al., 2015) older than 125 ka (Otte et al., 1998).

3. Anthropological settings

The Kocabaş skull was attributed to *Homo erectus* (Kappelman et al., 2008). It is composed of 3 fragments separated at the cranial sutures, which were not completely fused due to the young age of the specimen (Fig. 1). The three cranial fragments were scanned using the Philips helical scanner at the Pamukkale teaching hospital, in Denizli, on September 14th, 2009; slice thickness was 0.80 mm, the space between slices was 0.4 mm (field of view: 20 cm, matrix: 512 × 512, power: 175 mA, intensity: 120 kV).

A first virtual reconstruction was carried out based on the CT data (Vialet et al., 2011, 2012). This paper concerns the second virtual reconstruction with Geomagic Studio 12 software by A.V. and P.W. (technical platform ASIM, at the MNHN). In this reconstruction, called "Kocabaş 2", the right part of the frontal bone is more accurately situated. Indeed, there is a gap of a few millimeters between the parietal and frontal sutures which prevents the direct anatomical connection between the two bones, as was previously thought and consequently applied to the first reconstruction. This reconstruction proceeded as follows. First, the two parietal fragments (right and left) were rearticulated following the congruence of their sagittal suture. Such rearticulation could be done using different angles. To ensure that the rearticulated bones were not out of the initial volume, we confirmed that they are situated between the two reference

Fig. 1. Superior view of the three isolated fragments composing the Kocabaş fossil. a: the right part of the frontal bone; b: the left fronto-parietal part; c: the right parietal fragmentary bone.
Fig. 1. Vue supérieure des trois fragments osseux isolés qui composent le fossile de Kocabaş. a : la partie droite de l'os frontal ; b : la partie fronto-pariétale gauche ; c : l'os pariétal fragmentaire droit.

Table 1
Comparison of the measurements of the two reconstitutions of the Kocabaş skull.
Tableau 1
Comparaison des mesures des deux reconstitutions du crâne de Kocabaş.

Reconstitution	M10	M9	M43
Kocabaş 1 *From* Vialet et al., 2012	102	85	116
Kocabaş 2 *From* Vialet et al., 2014	106	88	118

planes (i.e. the cutting sections made by the blades of the machine shown by the exposure of diploic tissue at the central part of the frontal and posterior part of the parietals). Then, using the mirror-imaging technique, we duplicated the right part of the frontal bone to reconstruct the left one. Finally, the anterior block (made by the completed frontal) was connected to the posterior block (made by the rearticulated parietals) using as guidelines the sagittal suture and the frontal crest (Fig. 2).

To conclude, the two reconstructions are different. This is the reason why the measurements taken for each one are not exactly the same, resulting in a slightly larger skull for the Kocabaş 2 reconstruction (Table 1).

Based on several morphological changes of various size observed on the endocranial surface of the right frontal fragment, Kappelman and co-workers (Kappelman et al., 2008) argued for the presence of a *Leptomeningitis tuberculosa* (tuberculous meningitis). However, the validity of this diagnosis was refuted and critical comments were made by Roberts and co-workers (Roberts et al., 2009).

Complementary studies employing new macromorphological and micro-CT analysis on the endocranial lesions are ongoing in order to clarify their morphological aspect, especially by focusing on soft tissue imprints and their possible inner extension.

4. Material

Casts of the main fossil hominin skulls from the lower to upper Pleistocene in Africa, Asia, and Europe were considered in this study (Table 2). They are stored at the National Museum of Natural History in Paris. 28 skulls in total were included in the 2D morphometric analysis and among them, 20 were used for cladistic analysis (including Sts5 as the outgroup specimen).

5. Methods

5.1. 2D morphometry

Standard metrical measurements from Martin and Saller (1957) were used to characterize the development of the frontal bone (Table 3). Principal component analysis was generated by Past 3.1. software (Hammer et al., 2001).

5.2. Cladistic analysis

To investigate the phylogenetic relationships of the Kocabaş hominin, we carried out a cladistic analysis using the characters defined in Table 4. Quotation was done on the originals and casts of the fossil skulls and from the

Fig. 2. The virtual reconstruction of Kocabaş 2. From left to right: the 3 steps of the process: 1, putting together the two parietals; 2, mirroring the right part of the frontal to reconstruct the overall bone; 3, connecting the frontal and parietal parts; 4, to obtain the most complete reconstruction (Kocabaş 2).
Fig. 2. La reconstitution virtuelle de Kocabaş 2. De gauche à droite : les trois étapes du processus. 1, mise en connexion des deux pariétaux ; 2, reconstitution de l'ensemble du frontal, par image miroir de la partie droite ; 3, mise en connexion des parties frontale et pariétale ; 4, pour obtenir la reconstitution la plus complète (Kocabaş 2).

Table 2
List of the hominin fossils used in this study.
Tableau 2
Liste des homininés fossiles utilisés dans cette étude.

Provenience	N	Name	2D	Clad	Dating	Reference
Africa						
South Africa	2	Sterfontein				
		Sts 5		X	2.8–2.4	Schwartz et al., 1994
					2.16–2.05	Herries and Shaw, 2011
		Stw53		X	2.6–2 Ma	Kuman and Clarke, 2000
Kenya	6	Koobi Fora				
		KNM-ER1470	X	X	2.06 Ma	Joordens et al., 2013
		KNM-ER1813	X	X	1.78 Ma	Feibel et al., 2009
		KNM-ER3733	X	X	1.65 Ma	Mc Dougall et al., 2012
		KNM-ER3883	X	X	1.49–1.65 Ma	Feibel et al., 1989
		KNM-ER42700		X	1.55 Ma	Spoor et al., 2007
		KNM-OL45500		X	0.97–0.90 Ma	Potts et al., 2004
Tanzania	2	Olduvai				
		OH24		X	1.88 Ma	Hay, 1976
		OH9	X	X	1.5–1.4 Ma	Schwartz and Tattersall, 2003
Ethiopia	1	Daka-Bouri				
		BouVP2/66	X	X	1 Ma	Asfaw et al., 2002
Eritrea	1	Buia				
		UA31		X	1 Ma	Abbate et al., 1998
Zambia	1	Kabwe	X		> 125 Ka	Schwartz and Tattersall, 2003
Georgia	4	Dmanisi				
		D2280	X	X	1.77 Ma	Lordkipanidze et al., 2007
		D2282	X			
		D2700	X	X		
		D3444	X			
Turkey	1	Denizli Basin				
Asia		Kocabaş 2	X	X	1.6–1.2 Ma	Lebatard et al., 2014a, 2014b
Indonesia	5	Sangiran				
		S17	X	X	0.8 Ma	Sémah et al., 2010, Hyodo et al., 2011
		Sambungmacan				
		Sm3	X		0.5 Ka	Yokoyama et al., 2008
		Ngandong				
		Ng 5, 10, 12	X		150–27 Ka	Indriati et al., 2011
China	7	Yunxian				
		Yunxian IIR	X		936 Ka	Lumley and Tianyuan, 2008
		Zhoukoudian				
		ZKD3, 11, 12	X	X	780 ± 80 Ka	Shen et al., 2009
		Hulu cave				
		Nankin 1	X	X	641 ± 39 Ka	Bahain et al., 2017
		Hexian			412 ± 25 Ka	Grün et al., 1998
		Dali			270 Ka	Xiao et al., 2002
Europe						
Greece	1	Petralona	X		150–250 Ka	Grün, 1996
France	3	Arago 21-47	X		438 ± 31 Ka	Falguères et al., 2015
		LCAS–La Chappelle aux saints	X		MIS3-MIS4	Rendu et al., 2014
		LF1–La Ferrassie 1	X		54 ± 3 to 40 ± 2 Ka	Guérin et al., 2015
Total	34		28	19		

Table 3
Conventional measurements used in this study. M9.1 is only used for the cladistic analysis.
Tableau 3
Mesures conventionnelles utilisées dans cette étude. M9.1 a été utilisé uniquement dans l'analyse cladistique.

Conventional measurements	from Martin and Sallers 1957	Definitions
M9–Minimal frontal width		Between the two frontotemporals (ft)
M9.1–Postorbital breadth		Minimum postorbital breadth
M10–Maximal frontal width		On the coronal suture, between the two coronion (co)
M43–Superior facial width		Between the two fronto-malar-temporals (fmt)
Frontal bone length M29.2	chord of the cerebral part of the frontal bone	From supra-glabellar (sg) to bregma (b)

literature for KNM-ER42700 (Spoor et al., 2007), Buia UA 31 (Abbate et al., 1998, Bruner et al., 2016), Daka-Bouri BouVP 2/66 (Asfaw et al., 2002, 2008) and KNM-OL 45500 (Potts et al., 2004).

Eighteen characters of the frontal bone were used; 14 are morphological characters and 4 are metric characters. As there is no consensus on the taxonomic classification of numerous hominin specimens, we define the Operational

Table 4
Features used for the cladistic analysis.
Tableau 4
Caractères utilisés pour l'analyse cladistique.

Feature number	Description	References
1	Continuity of the postorbital groove *0: absent, 1: present but incomplete, 2: present continuously*	Zeitoun, 2000 (feature 4 p54)
2	Shape of the frontal superior border in superior view *0: straight, 1: convex*	Zeitoun, 2000 (feature 8 p56)
3	Height of the lateral part of the supra-orbital torus (c) in comparison with its central part (mid-orbital position) (b) *0: c > b, 1: c < b, 2: c = b*	Zeitoun, 2000 (modified from feature 12 p59)
4	Width of the temporal band (space between temporal lines) on the frontal bone *0: narrow, 1: large*	Zeitoun, 2000 (feature 13 p60)
5	Projection of the temporal band (space between temporal lines) on the frontal bone *0: flat, 1: prominent and strongly prominent*	Zeitoun, 2000 (feature 14 p60)
6	Bregmatic eminence overlapped on the parietal bone *0: absent, 1: present*	Zeitoun, 2000 (modified from feature 21 p62)
7	Supratrigonal depression (on the antero-medial border of the temporal line) *0: absent, 1: present*	Zeitoun, 2000 (feature 25 p65)
8	Height of the lateral part of the supra-orbital torus (metric) *0: weak, 1: developed, 2: strong*	Prat, 2000, 2004, 2005 (modified from feature 6 p165)
9	Development of the zygomatic process of the frontal bone (which forms the lateral border of the orbit) *0: short, 1: long*	Feature exclusive to this study
10	Proportion of the frontal scale (M29.2/M9.1) (metric) *0: short, 1: long, 2: very long*	Feature exclusive to this study
11	Postorbital constriction (M9/M43) (metric) *0: strong, 1: developed, 2: less developed*	Feature exclusive to this study
12	Frontal bone divergence (M9.1/M10) (metric) *0: very divergent, 1: divergent, 2: less divergent*	Feature exclusive to this study
13	Convexity of the external lateral wall of the frontal bone below the temporal lines *0: vertical, 1: convex*	Feature exclusive to this study
14	Sagittal keel on the anterior half of the sagittal suture *0: absent, 1: present*	Zeitoun, 2000 (modified from feature 27 p65)
15	Postcoronal depression *0: absent, 1: present*	Zeitoun, 2000 (feature 31 p66)
16	Discontinuity of the temporal lines at Stephanion *0: absent, 1: present*	Zeitoun, 2000 (feature 34 p67)
17	Temporal lines (superior and inferior) separated on the parietal bone *0: separated, 1: fused*	Feature exclusive to this study
18	Shape of the orbital roof *0: globular (short roof), 1: conical (long)*	Feature exclusive to this study

Taxonomic Unit (OTU) by the specimen or group of specimens rather than by the species (as often used). This approach has been used by Caparros (1997); Zeitoun (2000); Gilbert et al. (2003); Prat (2004, 2005); Cameron et al. (2004); Mounier and Caparros (2015); Mounier et al. (2016) and Zeitoun et al. (2016). Character polarity has been determined by rooting the outgroup. The polymorphism is coded as multiple states (0&1, 0&2, 1&2, 0&1&2) with the polymorphism option of the Paup 4.01 software (Swofford, 1998). The quantitative characters were coded using the method proposed by Thiele (1993) (after a logarithmic transformation of data, these latter being standardized using the formula $x_S = ((x\text{–min})/(\text{max}\text{–min})) \times n$; n = maximum number of ordered states allowable by the algorithm used (32 for PAUP). There has been considerable debate concerning methods of coding quantitative characters. The method of Thiele (1993) was used because it allows the coding of all characters in a similar manner. The data were computed in a non-arbitrary way to avoid any preconceived phylogenetic hypothesis. Most of these characters have been taken from Zeitoun (2000) and Prat (2000, 2004, 2005). Some of them have been defined in this study (Table 4). The characters have been coded on ten OTU and the allocation of the character state for each one is given in Table 5. The OTU are as follows: *Australopithecus africanus* (Sts5), which is the outgroup in the analysis; early *Homo* (which comprises some specimens commonly allocated to *Homo habilis* and *Homo rudolfensis*: OH 24, KNM-ER 1470; KNM-ER 1813; Stw 53); early African *Homo erectus*/*Homo ergaster* (KNM-ER 3733, KNM-ER 3883; OH 9, KNM-ER 42700); *Homo georgicus* (D2280 and D2282); late African *Homo erectus* (Buia UA 31, Daka-Bouri BouVP2/66, KNM-OL 45500); Kocabaş 2; Indonesian *Homo erectus* (Sangiran 17); Chinese *Homo erectus* (ZKD 3, 11,12; Nankin 1). Except the individuals from this latter group, Asian and European middle and upper pleistocene specimens were not considered, as our analysis is more focused on the relationships between the Kocabaş fossil and lower and early middle Pleistocene hominins.

Table 5
Character states coding by Operational Taxonomic Unit.
Tableau 5
Codage des états de caractères par unité taxinomique opérationnelle (OTU).

Character numbers	Kocabaş	D2700, D2280	OH24, KNM-ER1813, KNM-ER1470, Stw53	KNM-ER37333, KNM-ER3883, OH9, KNM-ER42700	Buia UA31, Daka Bouri BOUVP2/66, KNM-OL45500	Zhoukoudian 3, 11, 12, Nankin	S17	Sts 5
1	2	1	0&2	0&1&2	1&2	2	0	0
2	1	0&1	0&1	1	0&1	0&1	1	0
3	0	0&1	0&1	0&1&2	1	0&1&2	0	0
4	0	0	0&1	0&1	1	0	0	0
5	1	0	0&1	0&1	1	0	0	0
6	0	1	0	0	?	1	1	0
7	1	0	0&1	0&1	1	0&1	0	0
8	1	0	0	1	?	1	2	0
9	0	0	0&1	0&1	0	1	0	0
10	1	2	2	1	0	2	1	0
11	2	1	1	1	1	2	2	1
12	2	1	1	1	2	1	2	0
13	1	1	0&1	1	0	1	0	1
14	0	1	0	0&1	0	1	?	0
15	0	1	0	0	?	1	1	0
16	0	0	0	1	1	0	0	0
17	0	0&1	1	1	0	0&1	1	1
18	0	1	0	1	1	1	1	?

Table 6
Measurements on the frontal bones of 28 fossil hominins.
Tableau 6
Mesures sur les os frontaux de 28 homininés fossiles.

Locality	No. specimen	Measurements			
		M9	M10	M43	M29.2
Denizli – Turkey	Kocabaş 2	88	106	118	80
Kenya – KNM	ER 1813	66	88	93	64
	ER 1470	70	90	106	78
	ER3733	83	109	116	77
	ER3883	81	108	115	87
Tanzania – Olduvai	OH9	84	105	130	84
Georgia – Dmanisi	D3444	70	94	105	75
	D2280	74	106	114	86
	D2282	67	91	105	78
	D2700	67	90	97	71
Ethiopia – Daka-Bouri	BouVP2/66	89	105	124	75
China – Yunxian	YII Reconst.	102	136	130	74
China – Hulu cave	Nankin	83	101	110	80
China – Zhoukoudian	ZKD 3	81	105	109	90
	ZKD 11	84	106	111	90
	ZKD 12	91	110	119	97
Java – Sangiran	Sang 17	96	115	119	94
China	Hexian	96	116	111	76
France – Arago	Arago 21 Reconst.	109.1	113.1	123	92
Greece	Petralona	108	120	130	92
Zambia	Kabwe	98	117	133	105
China	Dali	103	121	123	101
Java – Sambungmacan	Sm 3	99	110	112	93
Java – Ngandong	Ng 5	100	121	116	97
	Ng 10	102	121	121	99
	Ng 12	103	117	123	95
France – La Chapelle-aux-Saints	LCAS	106	129	118	89
France – La Ferrassie	LF1	108	126	120	92

To bring to light the homoplasies and synapomorphies, we performed a parsimony analysis following the protocol developed by Miguel Caparros in Caparros (1997) and Mounier and Caparros (2015). A first low-level analysis is conducted with a branch and bound search in order to ascertain the phylogenetic information content of the character by its retention index. The retention index (RI) is calculated by subtracting the observed tree-length from the maximum possible tree-length and then dividing this value by the difference between the maximum and the minimum lengths (Archie, 1989; Farris, 1989). All characters are unordered and all have equal weight. In a

second step, 18 characters were reanalyzed after reweighting with the rescale consistency index (RC = CI (consistency index) × RI (retention index)). The consistency index (CI) is calculated as the minimum possible tree-length divided by the observed tree-length (Farris, 1989; Kluge and Farris, 1969). If there is no homoplasy in a tree, then its observed length equals the minimum tree-length and the CI equals one. If homoplasy is present, then the CI is less than one. We use the ACCTRAN method (which maximizes reversals) in order to resolve the ambiguities of the character changes at the hypothetical ancestor nodes, as it provides more character support to clades.

The most parsimonious trees were obtained using the heuristic search algorithm with the branch-swapping algorithm (TBR). We use PAUP version 4.01 (Swofford, 1998), and MacClade (v. 4.06) in order to illustrate the supporting characters at the hypothetical ancestor's nodes.

6. Results

6.1. Anthropological study–2D morphometry

Metrics are presented in Table 6.

The PCA was computed based on 4 variables (M9, M10, M43, M29.2) measured on 28 fossils. On the first axis (which accounts for 82.5% of the total variance), individuals are spread following their global size (Fig. 3). Kocabaş 2 is among the *Homo erectus s.l.* from Africa and Asia. The Dmanisi fossils are smaller and the *Homo heidelbergensis*, late *Homo erectus* and Neandertals are bigger.

On the second axis (11.3% of the total variance), the length of the frontal bone separates the fossils. Kocabaş 2 is distinct not only from the Zhoukoudian *Homo erectus* but also from Sangiran 17, OH9 and KNM-ER3883. It is closer to African fossils such as KNM-ER3733 and Daka-Bouri BouVP2/66 (Fig. 3) which show a relatively shorter frontal scale.

The distribution of the fossils across the third axis (4% of the total variance) is linked with the width of the supra-orbital torus (Fig. 4). Again, Kocabaş 2 is in an intermediate position between the Asian *Homo erectus* (Zhoukoudian with a gracile supra-orbital torus) and the African ones (OH9, Daka-Bouri BouVP2/66 with a strong supra-orbital torus). For this feature, the Turkish specimen is closer to the Dmanisi and the East Turkana (KNM-ER3733 and ER3883) specimens.

The weak divergence of the frontal bone (proportion between minimal-M9 and maximal-M10 frontal widths) is expressed on the fourth axis (2.1%), on which the Kocabaş 2 skull is far from the Asian and African *Homo erectus*, except OH9 (Fig. 5).

The results of this study allow us:

- to link Kocabaş 2 with early and late African *Homo erectus*;
- to distinguish it from the early *Homo* specimens and from the small Georgian hominins;
- to distinguish it from the Asian *Homo erectus*.

In comparison to the latter, Kocabaş 2 shows a shorter and posteriorly narrower frontal bone and a more prominent supra-orbital torus. With its small size, the Turkish skull is clearly distinct from the middle and upper Pleistocene hominins. Such results confirm the previous studies based on anatomical features and 3D morphometrics (Vialet et al., 2012, 2014).

6.2. Cladistic analysis

Concerning the phylogenetic analysis based on 18 characters and 7 specimens or group of specimens in the ingroup, three trees have been obtained on the first step of the analysis. The tree length is 31, consistency index (CI) = 0.7097; retention index (RI) = 0.5714; and rescaled consistency index (RC) = 0.4055.

A heuristic search based on 18 frontal features (Table 7), entered with equal weights, identified 9 morphological characters that contain phylogenetic information (RI ≥ 0.5). We identify 6 true synapomorphies (CI, RI, ad RC = 1, HI = 0); characters # 5 Projection of the temporal band on the frontal bone; # 6 Bregmatic eminence overlapped on the parietal bone; # 7 Supratrigonal depression; # 14 Sagittal keel on the anterior half of the sagittal suture; # 15 Postcoronal depression; # 17 Temporal lines separated on the parietal bone.

For the second step, we used a branch and bound algorithm to analyze the reweighted characters by respective RCs. Three trees have been obtained. The strict consensus tree is shown in Fig. 6. The tree length is 13.66, retention index (RI) = 0.8790; consistency index (CI) = 0.9051 and rescaled consistency index (RC) = 0.7956.

At Node A, the hypothetical ancestor of the group (Buia UA 31, Daka-Bouri BouVP2/66, OL 45500 and Kocabaş) is well supported by one synapomorphy (#17: superior and inferior temporal lines changing from fused to separated on the parietal bone, they do not form a strong ridge). This node is also supported by one informative homoplasy (# 12) frontal bone changing from divergent to less divergent.

Kocabaş exhibits the following informative characters (RI ≥ 0.5):

- # 5–Projection of the temporal band on the frontal bone (RI = 1): changes from flat to prominent and strongly prominent, which is shared with the group Buia UA 31, Daka-Bouri BouVP2/66, KNM-OL45500;
- # 7–Supratrigonal depression (RI = 1): changes from absent to present, which is shared with the group Buia UA 31, Daka-Bouri BouVP2/66, KNM-OL45500;
- # 8–Height of the lateral part of the supra-orbital torus (RI = 0.5): changes from weak to developed, which is shared with the group (KNM-ER 3733, 3883, 42700, OH9) and the group (Buia UA 31, Daka-Bouri BouVP2/66, KNM-OL45500) and a convergence with the hypothetical ancestor of the group (Zhoukoudian 3, 11, 12, Nankin 1) and Sangiran 17;
- # 11–Postorbital constriction (RI = 0.5): changes from developed to less developed which is a convergence with the hypothetical ancestor of Zhoukoudian 3, 11, 12, Nankin 1 and Sangiran 17. The decrease in postorbital constriction can be associated with increased flexion of the anterior cranial base (Cameron et al., 2004);
- # 12–Frontal bone divergence (RI = 0.5): changes from divergent to less divergent; this is shared with the group

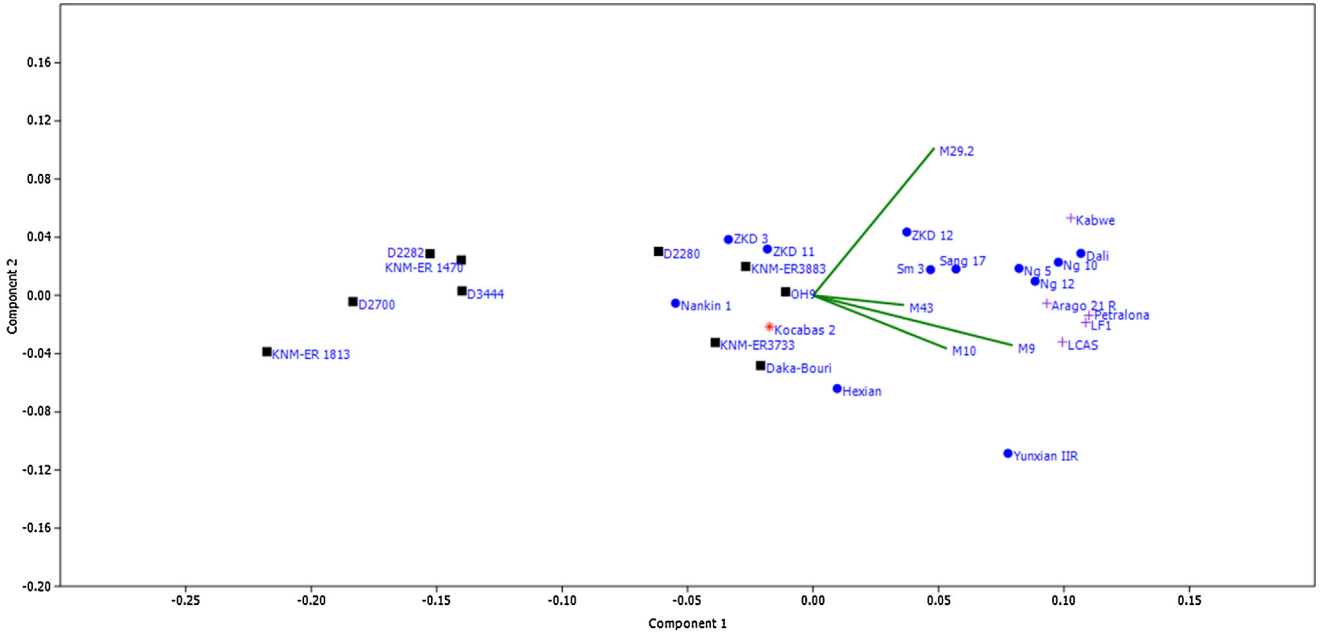

Fig. 3. PCA on 4 measurements on the frontal bone (M9, M10, M43, M29.2) from 28 hominins. Axis 1 accounts for 82.5% of the total variance and axis 2 for 11.3% of the total variance. Black squares: early *Homo* and African *Homo erectus*, blue dots: Asian *Homo erectus*, purple crosses: Middle Pleistocene European hominins and Neandertals, red star: the Kocabaş hominin.
Fig. 3. ACP sur quatre mesures de l'os frontal (M9, M10, M43, M29,2) sur 28 homininés. L'axe 1 compte pour 82,5 % de la variance totale et l'axe 2 pour 11,3 % de la variance totale. Carrés noirs : premiers *Homo* et *Homo erectus* africains ; points bleus : *Homo erectus* asiatiques ; croix violettes : homininés européens du Pléistocène moyen et Néandertaliens ; étoile rouge : l'homininé de Kocabaş.

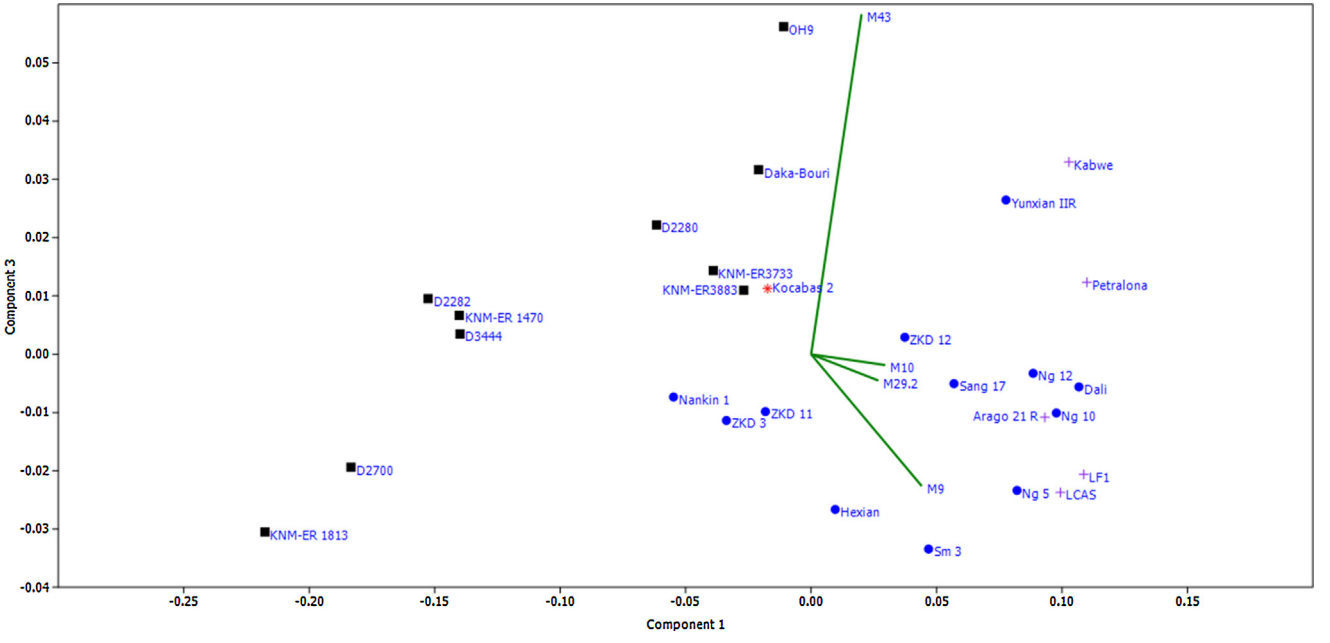

Fig. 4. PCA on 4 measurements on the frontal bone (M9, M10, M43, M29.2) from 28 fossils. Axis 1 accounts for 82.5% of the total variance and axis 3 for 4%. Black squares: early *Homo* and African *Homo erectus*, blue dots: Asian *Homo erectus*, purple crosses: Middle Pleistocene European hominins and Neandertals, red star: the Kocabaş hominin.
Fig. 4. ACP sur quatre mesures de l'os frontal (M9, M10, M43, M29,2) sur 28 homininés. L'axe 1 compte pour 82,5 % de la variance totale et l'axe 3 pour 4 %. Carrés noirs : premiers *Homo* et *Homo erectus* africains ; points bleus : *Homo erectus* asiatiques ; croix violettes : homininés européens du Pléistocène moyen et Néandertaliens, étoile rouge : l'homininé de Kocabaş.

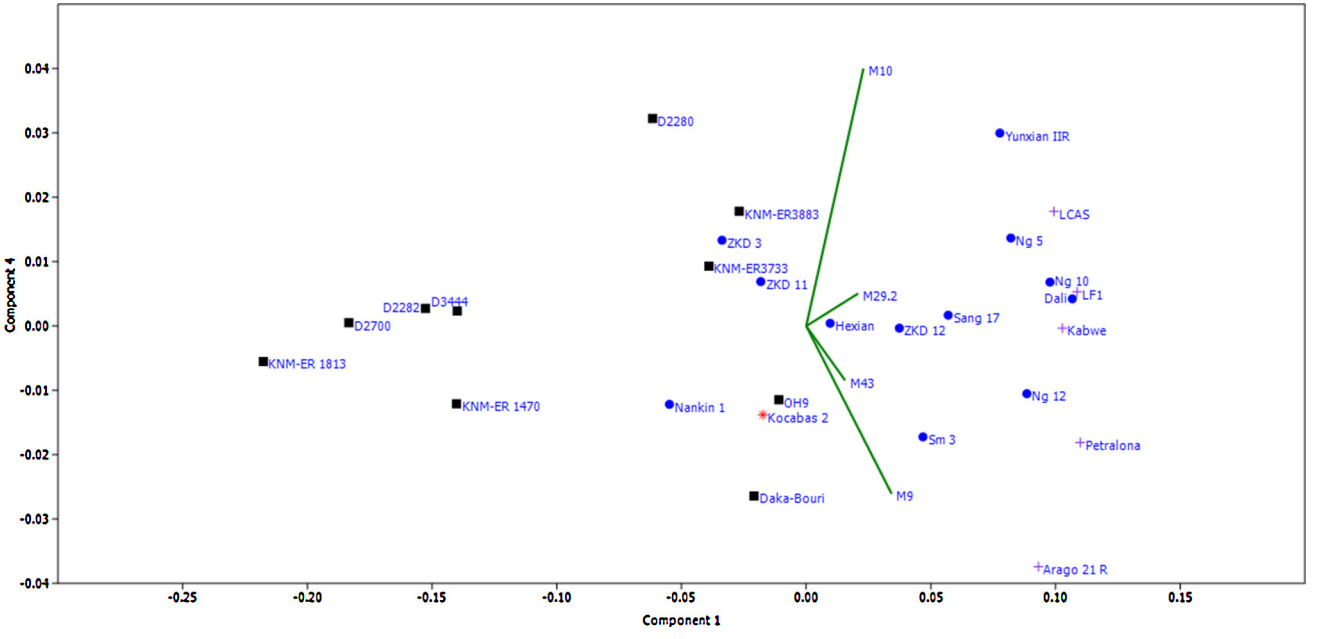

Fig. 5. PCA on 4 frontal bone measurements (M9, M10, M43, M29.2) from 28 fossils. Axis 1 accounts for 82.5% of the total variance and axis 4 for 2,1% of the total variance. Black squares: early *Homo* and African *Homo erectus*, blue dots: Asian *Homo erectus*, purple crosses: Middle Pleistocene European hominins and Neandertals, red star: the Kocabaş hominin.
Fig. 5. ACP sur quatre mesures de l'os frontal (M9, M19, M43, M29,2) sur 28 homininés. L'axe 1 compte pour 82,5 % de la variance totale et l'axe 4 pour 2,1 % de la variance totale. Carrés noirs : premiers *Homo* et *Homo erectus* africains ; points bleus : *Homo erectus* asiatiques ; croix violettes : homininés européens du Pléistocène moyen et Néandertaliens ; étoile rouge : l'homininé de Kocabaş.

Table 7
Character states coding.
Tableau 7
Codage des états de caractères.

Morhological features	Range	Minsteps	Treesteps	Maxsteps	CI	RI	RC	HI
1_Continuity of the postorbital groove	2	2	3	3	0.667	0.000	0.000	0.333
2_Shape of the frontal superior border in superior view	1	1	1	1	1.000	0/0	0/0	0.000
3_Height of the lateral part of the supra-orbital torus (c) in comparison with its central part (mid-orbital position) (b)	1	1	1	1	1.000	0/0	0/0	0.000
4_Width of the temporal band (space between temporal lines) on the frontal bone	1	1	1	1	1.000	0/0	0/0	0.000
5_Projection of the temporal band (space between temporal lines) on the frontal bone	1	1	1	2	1.000	1.000	1.000	0.000
6_Bregmatic eminence overlapped on the parietal bone	1	1	1	3	1.000	1.000	1.000	0.000
7_Supratrigonal depression (on the antero-medial border of the temporal line)	1	1	1	2	1.000	1.000	1.000	0.000
8_Height of the lateral part of the supra-orbital torus (metric)	2	2	3	4	0.667	0.500	0.333	0.333
9_Development of the zygomatic process of the frontal bone (which forms the lateral border of the orbit)	1	1	1	1	1.000	0/0	0/0	0.000
10_Proportion of the frontal scale (M29.2/M9.1)	2	2	4	5	0.500	0.333	0.167	0.500
11_Postorbital constriction (M9/M43)	1	1	2	3	0.500	0.500	0.250	0.500
12_Frontal bone divergence (M9.1/M10)	2	2	3	4	0.667	0.500	0.333	0.333
13_Convexity of the external lateral wall of the frontal bone below the temporal lines	1	1	2	2	0.500	0.000	0.000	0.500
14_Sagittal keel on the anterior half of the sagittal suture	1	1	1	2	1.000	1.000	1.000	0.000
15_Postcoronal depression	1	1	1	3	1.000	1.000	1.000	0.000
16_Discontinuity of the temporal lines at Stephanion	1	1	2	2	0.500	0.000	0.000	0.500
17_Temporal lines (superior and inferior) separated on the parietal bone	1	1	1	2	1.000	1.000	1.000	0.000
18_Shape of the orbital roof	1	1	2	2	0.500	0.000	0.000	0.500

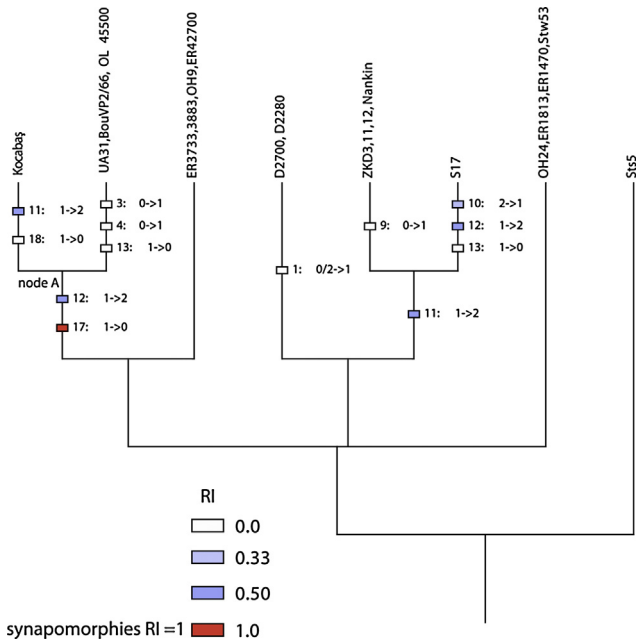

Fig. 6. Most Parsimonious Tree (MPT). Overall Retention Index RI = 0.8790; and Consistency Index CI = 0.9051.
Fig. 6. Arbre le plus parcimonieux. Indice de rétention général RI = 0,8790 ; indice de robustesse CI = 0,9051.

(Buia UA 31, Daka-Bouri BouVP2/66, KNM-OL45500) and a convergence with Sangiran 17;

- # 17–Temporal lines separated on the parietal bone (RI = 1): superior and inferior temporal lines separated on the parietal bone, they do not form a strong ridge, changing from fused to separated, which is shared with the group (Buia UA 31, Daka-Bouri BouVP2/66, KNM-OL45500).

Furthermore, the Kocabaş specimen shows a conical orbital roof (#18, CI = 0,5; RI = 0), which is also observed in the group (OH 24, KNM-ER 1813, 1470, Stw 53).

7. Discussion

Our multivariate analysis, based on the main measurements of the frontal bone, places the Kocabaş fossil in the *Homo erectus s. l.* group (i.e. Zhoukoudian and Nankin 1 from China, KNM-ER3733, KNM-ER3883 from East Africa and the late African *Homo erectus* such as OH9 and Daka-Bouri BouVP2/66). Its overall size is greater than that of early *Homo* and the Dmanisi specimens and smaller than Middle and Upper Pleistocene hominins. However, the Turkish fossil differs from the Asian *Homo erectus* by the shortness of its frontal scale which is close to the African fossils, KNM-ER3733 and Daka-Bouri BouVP2/66. In our opinion, this difference, dealing with the proportion of the frontal bone and its elongation, is a very significant feature linked with endocranial development. Our conclusions differ from Aytek and Harvati's, who argued for a closeness between the Kocabaş fossil and, not only the Chinese Zhoukoudian III specimen, but also European hominins such as Ceprano and Arago (Aytek and Harvati, 2016). It is important to recall that their analysis only focuses on the supra-orbital torus which is a strongly dimorphic area. However, it is true that the Kocabaş and Zhoukoudian III specimens are morphologically close for this anatomical region and they are not far from the European fossils, such as the Ceprano and Arago 21 fossils which have a primitive supra-orbital torus. Regarding this area, we must mention another divergence from previous studies. Indeed, we consider that Kappelman et al. (2008) over-estimated the supra-orbital torus breadth (124 mm *vs* 118 mm in this study) and height (min 16–max 19 *vs* max 13 in our own measurements), which led to overemphasis on the closeness of the Turkish fossil with the Middle Pleistocene hominins. However, we must keep in mind that only the lateral half of the supra-orbital torus on the Kocabaş fossil is preserved which means that it is not possible to know how developed the medial part was. For the width of the supra-orbital torus, our results show an intermediate position for the Kocabaş hominin between on the one hand, a gracile group composed of the Asian *Homo erectus* and most of the Dmanisi and early *Homo* specimens, and on the other hand, the more robust OH9 and Daka-Bouri BouVP2/66 skulls.

Finally, Kocabaş shares a weak frontal divergence with the one-million-year-old *Homo erectus*-like hominins from East Africa (OH9, Daka-Bouri BouVP2/66). This character distinguishes them from earlier hominins including the Dmanisi fossils. These results are corroborated by the cladistic analysis which considers morphological as well as metrical features. Our analysis clearly separates two clades: an Asian one (including the Dmanisi specimens) and an African one (including the Kocabaş fossil). It enables us to consider an evolutionary history for the Kocabaş fossil, filling a gap in this fossil record, which is distinct from that of the Dmanisi group and linked with the African *Homo erectus* known between 1.65 Ma (KNM-ER3733), 1.5 Ma (OH9) and around 1 Ma (KNM-OL 45,500, Daka-Bouri BouVP2/66, Buia UA 31). The Turkish specimen is the first representative of such a cluster outside Africa. Another group is represented by the Asian *Homo erectus* (Zhoukoudian and Nankin 1), which are in a same clade with the Dmanisi fossils showing an expansion toward the East, rooted at, at least, 1.77 Ma. However, a less marked postorbital constriction (#11) is a common feature between Kocabaş and the ancestor of the Asian *Homo erectus* group showing that they have reached a similar developmental stage. In the same way, the frontal bone divergence (#12) is less pronounced in Sangiran 17 and the group including Kocabaş, Buia UA 31, Daka-Bouri BouVP 2/66, and KNM-OL45500 which is a convergent trait due to endocranial development. But among these fossils, Kocabaş shows a convexity of the frontal wall below the temporal lines (#13) which is vertical in the others. In summary, even though the Asian *Homo erectus*, the one-million-old African specimens and the Turkish fossil belong to the same stage of cranial development, Kocabaş seems different to some extent. Moreover, in this specimen, the orbital roof forms, at the back, a vertical wall (#18) which suggests the orbital cavity to be short and globular, instead of long and conical as observed in general on fossil hominins and *Homo sapiens*. This pattern, observed on KNM-ER1813 and on Stw53 as far as this area is preserved, may be linked with the overall small size of these individuals and/or its anatomical age.

An expansion of the Kocabaş group representatives toward the west could be expected based on their geographical location. Key specimens to test this question are the fossils from the Atapuerca-Sima del Elefante site dated to 1.2 Ma (Carbonell et al., 2008; Bermúdez de Castro et al., 2011) and Orce dated to 1.4 Ma (Toro-Moyano et al., 2013). Unfortunately, the Turkish (frontal bone) and Spanish fossils (mandible, hand phalanx, fragment of femur for Sima del Elefante, deciduous tooth for Orce) are not strictly comparable in terms of skeletal representation. More suitable are the frontal and the parietal bones discovered in the Aurora stratum (TD6.2) in the Atapuerca-Gran Dolina site, dated to 0.9 Ma (Moreno et al., 2015). Indeed, ATD6-15 consists of a large portion of the frontal bone (better preserved on its right side) but showing post-mortem distortion (Arsuaga et al., 1999). As far as they can be compared, the Turkish and Spanish fossils show some similarities. On both, we can observe the same convexity of the orbital roof (character #18) as a globular/short roof (*vs* conical/long one). As we have seen previously, this feature appears interesting to highlight the peculiarity of Kocabaş in comparison with the other specimens even if the RI is low (< 0.5). Maybe this similarity between the Turkish and Spanish hominins is due to the young age of both individuals, as the former is considered a young adult (Vialet et al., 2012) and the latter close to puberty (Arsuaga et al., 1999). The parietal bone (ATD6-100/168) is also from a young

individual between 8 and 10 years old when *Homo sapiens* is used as the reference (Bruner et al., 2017). That is the reason why the comparison is limited due to considerations of growth patterns and the state of preservation (i.e. in Kocabaş, only the anterior half of the parietal is preserved).

8. Conclusion

The results of the anthropological analysis highlight that the reconstructed Kocabaş partial skull (Kocabaş 2) shows a conformation of its frontal bone which is distinct from the early *Homo* pattern and intermediate between that of Asian *Homo erectus* and African *Homo erectus*. Cladistically speaking, the Turkish fossil is clearly separated from the Dmanisi fossils and the Asian *Homo erectus*, which are grouped in the same clade. It is linked not only to the African *Homo erectus* bracketed between 1.49 and 1.65 Ma but also with the one-million-year-old African hominins such as the KNM-OL45500, Daka-Bouri BouVP2/66 and Buia UA 31 skulls. Due to the lack of consensus to name the latter specimens and, generally speaking, to define *Homo erectus*, we maintain the attribution of the Kocabaş hominin to this species in the broadest sense, while we can suggest that the Turkish fossil shares an evolutionary history more with the African groups than the Asian ones. Filling a paleoanthropological gap outside Africa, between 1.6 and 1.2 Ma, it may provide evidence of human dispersal through south-western Europe and the entire Mediterranean area.

Acknowledgements

The authors want to warmely thank Pr. Yves Coppens for his invitation in this special issue of C.R. Palevol dedicated to the “Hominins and tools. Expansions from Africa towards Eurasia”. Most of the contributions of this issue have benefited from the support of the Agence Universitaire de la Francophonie in the context of the session B52 of the XVIIe Congrès de l’Union Internationale des Sciences Préhistoriques et Protohistoriques- UISPP (2014, Burgos, Spain). This research is an emanation of the “First Homo in Turkey”, a scientific project led by A. Vialet and supported by the CNRS (PICS 2016-2018). We are grateful to Louise Byrne and Phil Glauberman for linguistic assistance. MCA is supported to the GEBİP grant (The Outstanding Young Scientist Award) given by the Turkish Academy of Sciences (TÜBA).

References

Abbate, E., Albianelli, A., Azzaroli, A., Benvenuti, M., Tesfamariam, B., Bruni, P., Cipriani, N., Clarke, R.J., Ficcarelli, G., Macchiarelli, R., Napoleone, G., Papini, M., Rook, L., Sagri, M., Medhin Tecle, T., Torre, D., Villa, I., 1998. A one-million-year-old *Homo* cranium from the Danakil (Afar) depression of Eritrea. Nature 393, 458–460.

Alçiçek, M.C., 2014. Historique de la découverte et des recherches sur la calotte crânienne d’*Homo erectus* archaïque de Kocabaş, bassin de Denizli, Anatolie, Turquie. L’Anthropologie 118, 11–15.

Alçiçek, H., Alçiçek, M.C., 2014. Contexte géographique et géologique du site de Kocabaş, Bassin de Denizli, Anatolie, Turquie. L’Anthropologie 118, 8–10.

Archie, J., 1989. Homoplasy excess ratios: new indices for measuring levels of homoplasy in phylogenetic systematics and a critique of consistency index. Syst. Zool. 38, 239–252.

Arsuaga, J.L., Martinez, I., Lorenzo, C., Gracia, A., Muñoz, A., Alonso, O., Gallego, J., 1999. The human cranial remains from Gran Dolina lower Pleistocene site (Sierra de Atapuerca, Spain). J. Hum. Evol. 37, 431–457.

Asfaw, B., Gilbert, W.E., Beyene, Y., Hart, W.K., Renne, P.R., WoldeGabriel, G., Vrba, E.S., White, T., 2002. Remains of *Homo erectus* from Bouri, Middle Awash. Ethiopia. Nature 416, 317–320.

Asfaw, B., Gilbert, W.H., Richards, G.D., 2008. *Homo erectus* cranial anatomy. In: Gilbert, W.H., Asfaw, B. (Eds.), *Homo erectus* Pleistocene Evidence from the Middle Awash, Ethiopia. University of California Press (458 pp.).

Aytek, A.I., Harvati, K., 2016. The human fossil record from Turkey. In: Harvati, C., Roksandic, M. (Eds.), Paleoanthropology of the Balkans and Anatolia. Human evolution and its context. Springer, pp. 79–91.

Bahain, J.J., Shao, Q., Han, F., Sun, X., Voinchet, P., Liu, C., Yin, G., Falguères, C., 2017. Contribution des méthodes ESR et ESR/U-Th à la datation de quelques gisements pléistocènes de Chine. L’Anthropologie 121 (3), 215–233.

Bermúdez de Castro, J.M., Martinón-Torres, M., Gómez-Robles, A., Prado-Simón, L., Martín-Francés, L., Lapresa, M., Olejniczak, A., Carbonell, E., 2011. Early Pleistocene human mandible from Sima del Elefante (TE) cave site in Sierra de Atapuerca (Spain): a comparative morphological study. J. Hum. Evol. 61, 1–11.

Boulbes, N., Mayda, S., Titov, V.V., Alçiçek, M.C., 2014. Les grands mammifères du Villafranchien supérieur des travertins du Bassin de Denizli (Sud-Ouest Anatolie, Turquie). L’Anthropologie 118, 44–73.

Bruner, E., Bondioli, L., Coppa, A., Frayer, D.W., Holloway, R.L., Libsekal, Y., Medin, T., Rook, L., Macchiarelli, R., 2016. The Endocast of the One-Million-Year-Old Human Cranium from Buia (UA 31), Danakil Eritrea. Am. J. Phys. Anthropol. 160, 458–468.

Bruner, E., Píšová, H., Martín-Francésa, L., Martinón-Torres, M., Arsuaga, J.L., Carbonell, E., Bermúdez de Castro, J.M., 2017. A human parietal fragment from the late Early Pleistocene Gran Dolina-TD6 cave site, Sierra de Atapuerca, Spain. C. R. Palevol 16, 71–81.

Cameron, D., Patnaik, R., Sahni, A., 2004. The phylogenetic significance of the Middle Pleistocene Narmada hominin cranium from central India. Int. J. Osteoarchaeol. 14, 419–447.

Caparros, M., 1997. *Homo sapiens* archaïques : un ou plusieurs (taxons) espèces ? Analyse cladistique et analyse morphométrique (Thèse). Museum National d’Histoire Naturelle de Paris.

Carbonell, E., Bermúdez de Castro, J.M., Parés, J.M., Pérez-González, A., Cuenca-Bescós, G., García, N., Granger, D.E., Huguet, R., van der Made, J., Martinón-Torres, M., Rodríguez, X.P., Rosas, A., Sala, R., Stock, G.M., Vallverdú, J., Vergés, J.M., Allué, E., Benito, A., Burjachs, F., Cáceres, I., Canals, A., Díez, J.C., Lozano, M., Mateos, A., Navazo, M., Rodríguez, J., Rosell, J., Arsuaga, J.L., 2008. The first hominin of Europe. Nature 452, 465–470.

Chevalier, T., Özçelik, K., de Lumley, M.A., Kosem, B., de Lumley, H., Yalçinkaya, I., Taşkıran, H., 2015. The endostructural pattern of a middle Pleistocene human femoral diaphysis from the Karain E site (southern Anatolia, Turkey). Am. J. Phys. Anthropol. 157, 648–658.

Dinçer, B., 2016. The Lower Paleolithic in Turkey: Anatolia and Hominin dispersal out of Africa. In: Harvati, C., Roksandic, M. (Eds.), Paleoanthropology of the Balkans and Anatolia. Human evolution and its context. Springer, pp. 213–228.

Falguères, C., Shao, Q., Han, F., Bahain, J.-J., Richard, M., Perrenoud, C., Moigne, A.-M., de Lumley, H., 2015. New ESR and U-series dating at Caune de l’Arago, France: a key-site for European Middle Pleistocene. Quat. Geochronol. 30, 547–553.

Farris, J.S., 1989. The retention index and the rescaled consistency index. Cladistics 5, 417–419.

Feibel, C.S., Brown, H., McDougall, I., 1989. Stratigraphic context of fossil hominids from the Omo group deposits: northern Turkana Basin, Kenya and Ethiopia. Am. J. Phys. Anthrop. 78, 595–622.

Feibel, C.S., Lepre, C.J., Quinn, R.L., 2009. Stratigraphy, correlation, and age estimates for fossils from Area 123, Koobi Fora. J. Hum. Evol. 57, 112–122.

Gilbert, W.H., White, T.D., Asfaw, B., 2003. *Homo erectus*, *Homo ergaster*, *Homo “cepranensis”* and the Daka cranium. J. Hum. Evol. 45, 255–259.

Grün, R., 1996. A re-analysis of electron spin resonance dating results associated with the Petralona hominid. J. Hum. Evol. 30, 227–241.

Grün, R., Huang, P., Huang, W., Dermott, F.M., Thorne, A., Stringer, C.B., Yan, G., 1998. ESR and U-series analyses of teeth from the palaeoanthropological site of Hexian, Anhui Province, China. J. Hum. Evol. 34, 555–564.

Güleç, E., White, T., Kuhn, S., Özer, I., Sağır, M., Yilmaz, H., Howell, F.C., 2009. The Lower Pleistocene lithic assemblage from Dursunlu (Konya), central Anatolia, Turkey. Antiquity 83, 11–22.

Guérin, G., Frouin, M., Talamo, S., Aldeias, V., Bruxelles, L., Chiotti, L., Dibble, H.L., Goldberg, P., Hublin, J.-J., Jain, M., Lahaye, Ch., Madelaine, S., Maureille, B., McPherron, S.P., Mercier, N., Murray, A.S., Sandgathe, D., Steele, T.S., Thomsen, K.J., Turq, A., 2015. A multi-method luminescence dating of the Palaeolithic sequence of La Ferrassie based on new excavations adjacent to the La Ferrassie 1 and 2 skeletons. J. Archaeol. Sci. 58, 147–166.

Hammer, Ø., Harper, D.A.T., Ryan, P.D., 2001. PAST: paleontological statistics software package for education and data analysis. Paleontologia Electronica 4 (1), 1–9.

Hay, R.L., 1976. In: The Geology of Olduvai, Gorge, Hay, R.L. (Eds.), The setting of the gorge and history of the geological investigations. University of California Press, Berkeley, pp. 25–28.

Herries, A.I.R., Shaw, J., 2011. Palaeomagnetic analysis of the Sterkfontein palaeocave deposits: implications for the age of the hominin fossils and stone tool industries. J. Hum. Evol. 60, 523–539.

Howell, F.C., Arsebük, G., Kuhn, S., 1996. The Middle Pleistocene lithic assemblage from Yarimburgaz cave Turkey. Paléorient 22 (1), 31–49.

Hyodo, M., Matsu'ura, S., Kamishima, Y., Kondo, M., Takeshita, Y., Kitaba, I., Danhara, T., Aziz, F., Kurniawan, I., Kumai, H., 2011. High-resolution record of the Matuyama-Brunhes transition. Constrains the age of javanese *Homo erectus* in the Sangiran dome, Indonesia. Proc. Natl. Acad. Sci. USA 108, 19563–19568.

Indriati, E., Swisher III, C.C., Lepre, C., Quinn, R.L., Suriyanto, R.A., Hascaryo, A.T., Grün, R., Feibel, C.S., Pobiner, L., Aubert, M., Lees, W., Anton, S.C., 2011. The age of the 20 meter Solo river terrace, Java, Indonesia and the survival of *Homo erectus* in Asia. PLoS One 6 (6), e21562.

Joordens, J.C.A., Dupont-Nivet, G., Feibel, C.S., Spoor, F., Sier, M.J., van der Lubbe, J.H.J.L., Trine Kellberg Nielsen, T.K., Knul, M.V., Davies, G.R., Vonhof, H.B., 2013. Improved age control on early *Homo* fossils from the upper Burgi Member at Koobi Fora, Kenya. J. Hum. Evol. 65, 731–745.

Kappelman, J., Alçiçek, M.C., Kazanci, N., Schultz, M., Özkul, M., Şen, Ş., 2008. First *Homo erectus* from Turkey and implications for migrations into temperate Eurasia. Am. J. Phys. Anthropol. 135, 110–116.

Khatib, S., Rochette, P., Alçiçek, M.C., Lebatard, A.E., Demory, F., Saos, T., 2014. Études stratigraphique, sédimentologique et paléomagnétique des travertins de Kocabaş, Bassin de Denizli, Anatolie, Turquie, contenant des restes fossiles quaternaires. L'Anthropologie 118, 16–33.

Kluge, A.C., Farris, J.S., 1969. Quantitative phyletics and the evolution of the anurans. Syst. Zool. 18, 1–32.

Kuman, K., Clarke, R.J., 2000. Stratigraphy, artefact industries and hominid associations for Sterkfontein, Member 5. J. Hum. Evol 38, 827–847.

Lebatard, A.-E., Alçiçek, M.C., Rochette, P., Khatib, S., Vialet, A., Boulbes, N., Bourlès, D.L., Demory, F., Guipert, G., Mayda, S., Titov, V.V., Vidal, L., de Lumley, H., 2014a. Dating the *Homo erectus* bearing travertine from Kocabaş (Denizli, Turkey) at least 1.1 Ma. Earth Planet. Sci. Lett. 390, 8–18.

Lebatard, A.E., Bourlès, D.L., Alçiçek, M.C., 2014b. Datation des travertins de Kocabaş par la méthode des nucléides cosmogéniques $^{26}Al/^{10}Be$. L'Anthropologie 118, 34–43.

Lordkipanidze, D., Jashashvili, T., Vekua, A., Ponce de León, M.S., Zollikofer, C.P.E., Rightmire, G.P., Pontzer, H., Ferring, R., Oms, O., Tappen, M., Bukhsianidze, M., Agusti, J., Kahlke, R., Kiladze, G., Martinez-Navarro, B., Mouskhelishvili, A., Nioradze, M., Rook, L., 2007. Postcranial evidence from early *Homo* from Dmanisi, Georgia. Nature 442, 305–310.

de Lumley, H., Tianyuan, L., 2008. Le site de l'Homme de Yunxian. CNRS Éditions et Editions Recherche sur les civilisations, Quyuanhekou, Quingqu, Yunxian, Province du Hubei, Chine (587 p.).

Mc Dougall, I., Brown, F.H., Casconcelos, P.M., Cohen, B.E., Thiede, D.S., Buchanan, M.J., 2012. New single crystal $^{40}Ar/^{39}Ar$ ages improve time scale for deposition of the Omo Group, Omo–Turkana Basin, East Africa. J. Geol. Soc. 169, 213–226.

Maddy, D., Schreve, D., Demir, T., Veldkamp, A., Wijbrans, J.R., van Gorp, W., van Hinsbergen, D.J.J., Dekkers, M.J., Scaife, R., Schoorl, J.M., Stemerdink, C., van der Schriek, T., 2015. The earliest securely-dated hominin artefact in Anatolia? Quat. Sci. Rev. 109, 68–75.

Martin, R., Saller, K., 1957. Lehrbuch der Anthropologie, vol. 1/7. Gustav Fischer Verlag, Stuttgart (661 pp.).

Moreno, D., Falguères, C., Perez-Gonzalez, A., Voinchet, P., Ghaleb, B., Despriée, J., Bahain, J.J., Sala, R., Carbonell, E., Bermúdez de Castro, J.M., Arsuaga, J.L., 2015. New radiometric dates on the lowest stratigraphical section (TD1 to TD6) of Gran Dolina site (Atapuerca, Spain). Quat. Geochronol. 30, 535–540.

Mounier, A., Caparros, M., 2015. The phylogenetic status of *Homo heidelbergensis* – a cladistic study of Middle Pleistocene hominins. Bull. Mem. Soc. Anthropologie Paris 27, 110–134.

Mounier, A., Balzeau, A., Caparros, M., Grimaud-Hervé, D., 2016. Brain, calvarium, cladistics: a new approach to an old question, who are modern humans and Neandertals? J. Hum. Evol. 92, 22–36.

Otte, M., Yalçinkaya, I., Kozlowski, J., Bar-Yosef, O., López Bayón, I., Taşkıran, H., 1998. Long-term technical evolution and human remains in the Anatolian Palaeolithic. J. Hum. Evol. 34, 413–431.

Potts, R., Behrensmeyer, A.K., Deino, A., Ditchfield, P., Clark, J., 2004. Small Mid-Pleistocene Hominin Associated with East African Acheulean Technology. Science 305, 75–78.

Prat, S., 2000. Origine et taxinomie des premiers représentants du genre *Homo* (Thèse). Université de Bordeaux I, Talence, France (Vol. 1, 587 p., Vol. 2, 100 p.).

Prat, S., 2004. Les premiers représentants du genre *Homo*, en quête d'une identité. Apports de l'étude morphologique et de l'analyse cladistique. Bull. Mem. Soc. Anthropol. Paris 16 (1–2), 17–35.

Prat, S., 2005. Characterising early *Homo*. In: From tools to, symbols., In: Backwell, L., D'errico, F. (Eds.), From hominids to modern humans. Witwatersrand University Press, Johannesburg, pp. 198–228.

Prat, S., 2017. First settlements out of Africa: Tempo and dispersal mode: review and perspectives. C. R. Palevol, http://dx.doi.org/10.1016/j.crpv.2016.04.009 (this issue).

Rendu, W., Beauval, C., Crevecoeur, I., Bayle, P., Balzeau, A., Bismuth, T., Bourguignon, L., Delfour, G., Faivre, J.P., Lacrampe-Cuyaubère, F., Tavorminac, C., Todisco, D., Turq, A., Maureille, B., 2014. Evidence supporting an intentional Neandertal burial at La Chapelle-aux-Saints. Proc. Natl. Acad. Sci. USA 111, 81–86.

Roberts, C.A., Pfister, L.A., Mays, S., 2009. Letter to the Editor: Was Tuberculosis present in *Homo erectus* in Turkey? Am. J. Phys. Anthropol. 139, 442–444.

Sémah, A.M., Sémah, F., Djubiantono, T., Brasseur, B., 2010. Landscapes and hominids' environments: changes between the Lower and the early Middle Pleistocene in Java (Indonesia). Quat. Int. 223-224, 451–454.

Schwartz, J.H., Grün, R., Tobias, P.V., 1994. ESR dating studies of the Australopithecine site of Sterkfontein, South Africa. J. Hum. Evol. 26, 175–181.

Schwartz, J.H., Tattersall, I., 2003. The Human Fossil Record. Craniodental Morphology of Genus *Homo* (Africa and Asia), Vol. 2. Wiley-Liss, New York (603 p.).

Shen, G., Gao, X., Gao, B., Granger, D.E., 2009. Age of Zhoukoudian *Homo erectus* determined with $^{26}Al/^{10}Be$ burial dating. Nature 458, 198–200.

Slimak, L., Roche, H., Mouralis, D., Buitenhuis, H., Balkan-Atli, N., Binder, D., Kuzucuoğlu, C., Grenet, M., 2004. Kaletepe Deresi 3 (Turquie), aspects archéologiques, chronologiques et paléontologiques d'une séquence pléistocène en Anatolie centrale. C. R. Palevol 3, 411–420.

Slimak, L., Kuh, S.L., Roche, H., Mouralis, D., Buitenhuis, H., Balkan-Atlı, N., Binder, D., Kuzucuoğlu, C., Guillou, H., 2008. Kaletepe Deresi 3 (Turkey): archaeological evidence for early human settlement in Central Anatolia. J. Hum. Evol. 54, 99–111.

Spoor, F., Leakey, M.G., Gathogo, P.N., Brown, F.H., Anton, S.C., McDougall, I., Kiarie, C., Manthi, F.K., Leakey, L.N., 2007. Implications of new early *Homo* fossils from Ileret, east of Lake Turkana, Kenya. Nature 448, 688–691.

Swofford, D.L., 1998. PAUP phylogenetic analysis using parsimony, version 4.01.s. In: Computer program. Illinois Natural History Survey, Champaign, Illinois, USA.

Taşkıran, H., 2008. Réflexions sur l'Acheuléen d'Anatolie. L'Anthropologie 112, 140–158.

Taşkıran, H., 2018. The distribution of Acheulean culture and its possible routes in Turkey. C. R. Palevol. 17, http://dx.doi.org/10.1016/j.crpv.2016.12.005 (this issue).

Thiele, K., 1993. The holy of the perfect character: the cladistics treatment of morphometric data. Cladistics 9, 275–304.

Toro-Moyano, I., Martínez-Navarro, B., Agustí, J., Souday, C., Bermúdez de Castro, J.M., Martinón-Torres, M., Fajardo, B., Duval, M., Falguères, C., Oms, O., Parés, J.M., Anadon, P., Julia, R., Garcia, Aguilar, J.M., Moigne, A.M., Espigares, M.P., Rosmontoya, S., Palmqvist, P., 2013. The oldest human fossil in Europe, from Orce (Spain). J. Hum. Evol. 65 (1), 1–9.

Tryon, C.A., Logan, M.A.V., Mouralis, D., Kuhn, S., Slimak, L., Balkan-Atlı, N., 2009. Building a tephrostratigraphic framework for the Paleolithic of Central Anatolia, Turkey. J. Archaeol. Sci. 36 (3), 637–652.

Vialet, A., Guipert, G., Alçiçek, M.C., 2011. Reconstitution 3D et étude de l'*Homo erectus* de Kocabaş, en Turquie. Bull. Mem. Soc. Anthropol. Paris 23, S38.

Vialet, A., Guipert, G., Alçiçek, M.C., 2012. *Homo erectus* found still further west: reconstruction of the Kocabaş cranium (Denizli, Turkey). C. R. Palevol 11, 89–95.

Vialet, A., Guipert, G., Alçiçek, M.C., de Lumley, M.-A., 2014. La calotte crânienne de l'*Homo erectus* de Kocabaş (Bassin de Denizli, Turquie). L'Anthropologie 118, 74–107.

Villmoare, B., Kimbel, W.H., Seyoum, C., Campisano, C.J., Dimaggio, E.N., Rowan, J., Braun, D.R., Arrowsmith, J.R., Reed, K.E., 2015. Early *Homo* at 2.8 Ma from Ledi-Geraru, Afar, Ethiopia. Science 347, 1352–1355.

Xiao, J., Jin, C., Zhu, Y., 2002. Age of the fossil Dali man in northcentral China deduced from chronostratigraphy of the loess paleosol sequence. Quat. Sci. Rev. 21, 2191–2198.

Yokoyama, Y., Falguères, C., Sémah, F., Jacob, T., Grün, R., 2008. Gamma-ray spectrometric dating of late *Homo erectus* skulls from Ngandong and Sambungmacan, Central Java, Indonesia. J. Hum. Evol. 55, 274–277.

Zeitoun, V., 2000. Révision de l'espèce *Homo erectus* (Dubois, 1893). Utilisation des données morphologiques et métriques en cladistique, reconsidération du cas *Homo erectus*. Bull. Mem. Soc. Anthropologie Paris 12 ns 1–2, 1–200.

Zeitoun, V., Barriel, V., Widoanto, H., 2016. Phylogenetic analysis of the calvaria of *Homo floresiensis*. C.R. Palevol 15, 555–568.